ARTICLE IN PRESS

European Journal of Mechanics B/Fluids ▮ (▮▮▮▮) ▮▮▮–▮▮▮

Contents lists available at SciVerse ScienceDirect

European Journal of Mechanics B/Fluids

journal homepage: www.elsevier.com/locate/ejmflu

Respiratory effects on hemodynamics in patient-specific CFD models of the Fontan circulation under exercise conditions

Alessia Baretta [a], Chiara Corsini [a], Alison L. Marsden [b], Irene E. Vignon-Clementel [c], Tain-Yen Hsia [d], Gabriele Dubini [a], Francesco Migliavacca [a], Giancarlo Pennati [a,*]
The Modeling Of Congenital Hearts Alliance (MOCHA)[1]

[a] *Laboratory of Biological Structure Mechanics, Structural Engineering Department, Politecnico di Milano, Milan, Italy*
[b] *Mechanical and Aerospace Engineering Department, UCSD, CA, USA*
[c] *INRIA Paris-Rocquencourt, Le Chesnay, France*
[d] *Great Ormond Street Hospital for Children, London, UK*

ARTICLE INFO

Article history:
Available online xxxx

Keywords:
Computational fluid dynamics
Mathematical models
Multiscale model
Lumped-parameter
Congenital heart disease

ABSTRACT

Single ventricle malformations are complex congenital heart defects which require a three-stage surgical treatment, starting from the very first days of life, to separate the systemic and pulmonary circulations, and restore the serial circuit occurring in normal patients. The final surgery results in a total cavopulmonary connection (TCPC), where both the superior and the inferior vena cava are connected to the right pulmonary artery. Several clinical and computational studies have been done to optimize the geometry of the TCPC, with the aim of minimizing energy losses and improving surgical outcomes. To date, only few modeling studies have taken into account respiration and exercise as important factors to quantify the performance of a Fontan geometry.

The objective of this work is to test the dependence of fluid dynamic variables and energy efficiency on respiration in patient-specific models of Fontan circulation, when subjected to exercise tests.

A closed-loop multiscale approach was used, including a simple respiration model that modulates the extravascular pressures in the thoracic and abdominal cavities, to generate physiologic time-varying flow conditions. A lumped parameter network (LPN) representing the whole circulation was coupled to a patient-specific 3D finite volume model of the preoperative bidirectional cavo-pulmonary anastomosis (BCPA) with detailed pulmonary anatomy. Subsequently, three virtual TCPC alternatives were coupled to the LPN and investigated in terms of both local and global hemodynamics. In particular, a T-junction of the venae cavae to the pulmonary arteries, a design with an offset between the venae cavae and a Y-graft design were compared under exercise conditions.

Results showed that the BCPA model is able to realistically capture oscillations due to both cardiac and respiratory effects, when compared to the venous Doppler velocity tracings acquired preoperatively on the patient.

The differences in hemodynamics between the three investigated TCPC options were minimal and similar to those obtained without inclusion of respiratory effects. Hence, the three surgical options result to be equivalent according to the analyzed parameters.

Moreover, although the simulation of the Fontan circulation with a respiratory model requires a longer computational time, the developed framework allows for a more physiologic method to incorporate respiratory effects that was not possible using other methods.

* Correspondence to: Laboratory of Biological Structure Mechanics, Structural Engineering Department, Politecnico di Milano, Piazza Leonardo da Vinci, 32, 20133 Milan, Italy. Tel.: +39 02 2399 4223; fax: +39 02 2399 4386.
E-mail address: giancarlo.pennati@polimi.it (G. Pennati).

[1] MOCHA Investigators: Andrew Taylor, MD, Alessandro Giardini, MD, Sachin Khambadkone, MD, Silvia Schievano, PhD, Marc de Leval, MD, and T.-Y. Hsia, MD (Institute of Child Health, London, United Kingdom); Edward Bove, MD, and Adam Dorfman, MD (University of Michigan, Ann Arbor, MI); G. Hamilton Baker, MD, and Anthony Hlavacek (Medical University of South Carolina, Charleston, SC); Francesco Migliavacca, PhD, Giancarlo Pennati, PhD, and Gabriele Dubini, PhD (Politecnico di Milano, Milan, Italy); Alison Marsden, PhD (University of California, San Diego, CA); Jeffrey Feinstein, MD (Stanford University, Stanford, CA) Irene Vignon-Clementel (National Institute of Research in Informatics and Automation, Paris, France); Richard Figliola, PhD, and John McGregor, PhD (Clemson University, Clemson, SC).

0997-7546/$ – see front matter © 2012 Elsevier Masson SAS. All rights reserved.
doi:10.1016/j.euromechflu.2012.01.012

Please cite this article in press as: A. Baretta, et al., Respiratory effects on hemodynamics in patient-specific CFD models of the Fontan circulation under exercise conditions, European Journal of Mechanics B/Fluids (2012), doi:10.1016/j.euromechflu.2012.01.012

Nomenclature

$AR(t)$	Respiratory activation function
BCPA	Bidirectional cavo-pulmonary anastomosis
CO	Cardiac output
f_r	Respiratory frequency
HV	Hepatic vein
LPA	Left pulmonary artery
LPM	Lumped-parameter model
LPN	Lumped-parameter network
IVC	Inferior vena cava
O-TCPC	Total cavo-pulmonary anastomosis with offset
PFI	Pulsatility flow index
PVR	Pulmonary vascular resistances
RPA	Right pulmonary artery
SV	Single ventricle
SVC	Superior vena cava
SVR	Systemic vascular resistances
T-TCPC	T-shaped total cavo-pulmonary anastomosis
Y-TCPC	Total cavo-pulmonary anastomosis with Y-graft

1. Introduction

Complex congenital heart diseases are usually fatal within the first days or months of life, unless treated surgically. Single ventricle (SV) defects, such as hypoplastic left heart syndrome and tricuspid atresia, consist of only one functional ventricle and require a three-staged surgical approach, called the 'Fontan procedure', to separate the systemic and pulmonary circulations [1]. In stage one (Norwood or variant thereof) the aortic arch is reconstructed and a shunt is inserted to connect the systemic and pulmonary circulations, providing a means of blood oxygenation through a system of parallel pulmonary and systemic circulations (Fig. 1a). The second stage consists of a bidirectional cavopulmonary anastomosis (BCPA), in which the superior vena cava (SVC) is connected to the right pulmonary artery (RPA), with a "T-shaped" anastomosis (Fig. 1b), resulting in the upper systemic circulation being in series with the pulmonary one. The final stage consists of a total cavopulmonary connection (TCPC), connecting the inferior vena cava (IVC) to the RPA, resulting in a series circuit of systemic and pulmonary circulations (Fig. 1c). The final univentricular configuration restores the circuit occurring in normal patients, where the heart pumps blood to the pulmonary and systemic districts in sequence, although in the healthy circulation two ventricles are functioning (right RV and left LV ventricles, Fig. 1d).

The typical cross-shaped junction of the TCPC leads to unusual hemodynamic conditions that are not known to occur naturally in any region of the circulatory system. For this reason, in the last decade many clinical and computational fluid dynamic (CFD) studies were carried out on Fontan circulation to optimize the geometry of the connection, which is considered to be one of the major causes of energy losses and poor surgical outcomes.

Moreover, the flows entering the connection, namely SVC and IVC flows, exhibit complex waveforms due to the combined effects of cardiac contractility and respiratory modulation. Nonetheless, the first computational studies on the TCPC, carried out in the early 90's, used steady-state flows as boundary conditions, thus preventing physiologic representation of these phenomena. So far, most CFD studies using time-varying caval inflow boundary conditions have not taken into account the role of respiration on the local hemodynamics [2,3].

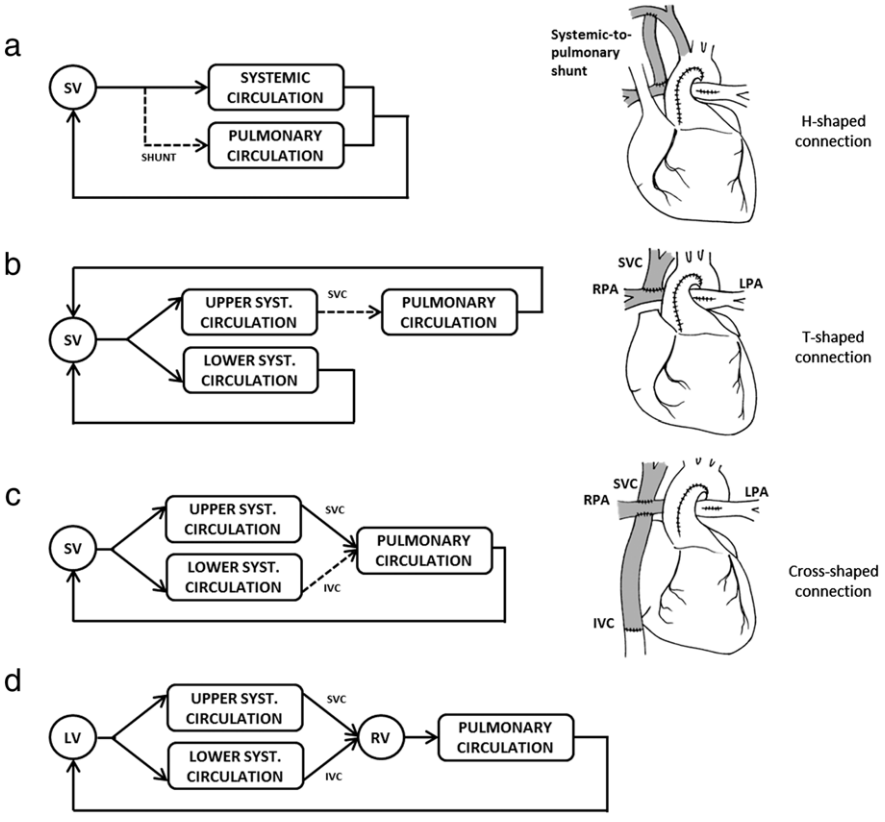

Fig. 1. Schematics of (a) *in parallel* Norwood circulation, with the interposition of a systemic-to-pulmonary shunt to deliver blood to the lungs; (b) BCPA circulation with upper systemic and pulmonary circulations *in series*; (c) Fontan circulation, with an *in series* circuit of systemic and pulmonary circulations; (d) *serial* normal circulation. The H-shaped, T-shaped and cross-shaped connections in BCPA and TCPC, respectively, are illustrated.

Please cite this article in press as: A. Baretta, et al., Respiratory effects on hemodynamics in patient-specific CFD models of the Fontan circulation under exercise conditions, European Journal of Mechanics B/Fluids (2012), doi:10.1016/j.euromechflu.2012.01.012

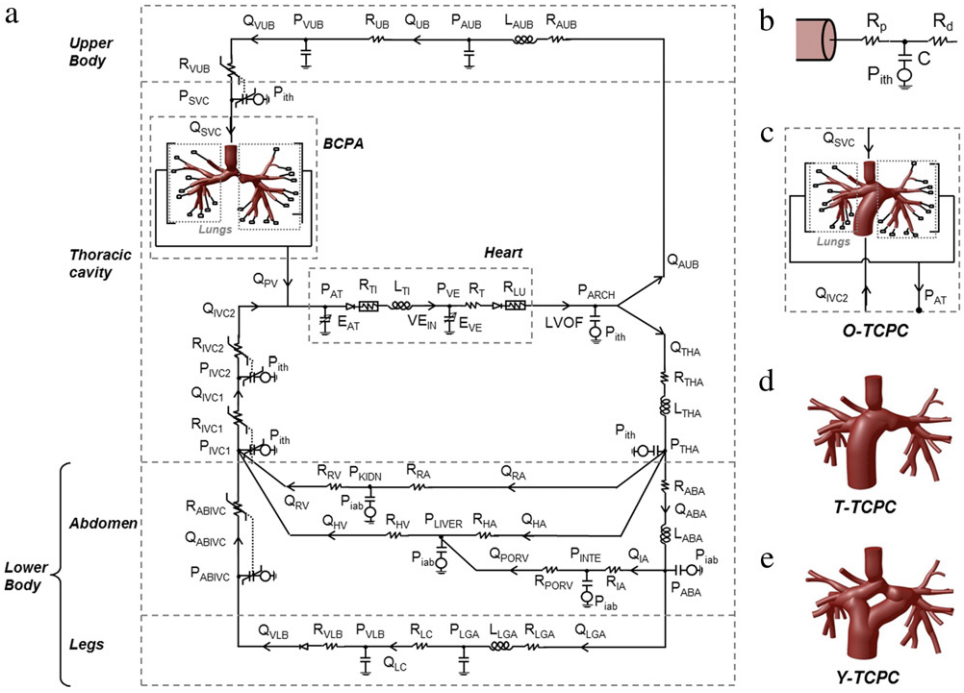

Fig. 2. (a) 3D–0D coupling of the LPM with the BCPA 3D model; (b) patient-specific RCR blocks connecting the outlets of the 3D models to the single atrium; post-operative 3D TCPC models: (c) O-TCPC showing the coupling with the LPM, (d) T-TCPC, (e) Y-TCPC.

More recent studies have shown the importance of respiration effects in the fluid dynamics of the intra-thoracic system, both on physiology and higher stress states with augmented flows and heart rate, such as exercise [4–6]. Furthermore, the interactions of caval flows in the cavopulmonary connection, including flow competition and phase shift, have been investigated in presence of the respiration [7].

When exercise conditions are simulated, hemodynamics are significantly altered, thus potentially lowering the efficiency of a geometry which may perform well at rest. Recent studies of Marsden et al. [4,6,8] performed simulations under exercise conditions in Fontan patients, adopting patient-specific caval flows with an superimposed respiratory waveform as TCPC inflow boundary conditions. These studies demonstrated that higher exercise flow rates led to increased energy losses, elevated pressure levels, and increased wall shear stress. Differences between designs were accentuated during exercise, which may correlate with the limited exercise capacity observed clinically in some TCPC patients. High stress states are therefore believed to be important conditions to quantify the performance and postoperative outcome of a particular Fontan geometry. However, these studies took into account the respiration in a very simple way by imposing pre-determined inflow conditions built ad hoc.

By using a closed-loop multiscale approach, where boundary conditions at inlet and outlet sections of the 3D model are directly calculated and imposed by the lumped-parameter model (LPM) [9], we previously demonstrated [10] that the TCPC configuration plays a minor role in the cardiac workload even during exercise. However, respiratory effects were not previously accounted for. Conversely, in the present work the effects of respiratory diaphragmatic motion on the hemodynamics of the cavopulmonary connection are investigated in the same patient-specific configurations of the previous study. Namely, we aim at obtaining respiratory modulated flow tracings in a more physiological way by simulating pressure changes in the abdominal and thoracic cavities.

The objectives of this work are thereby two: (i) to verify the possibility of reproducing the clinically observed venous flow tracings in Fontan patients through the inclusion of respiratory effects in previously developed closed-loop multiscale models and (ii) to evaluate the dependence of performance and energy efficiency on respiration in patient-specific models of the Fontan circulation, when subjected to exercise conditions.

2. Materials and methods

A closed-loop multiscale approach was used to couple two different models of blood circulation, namely a 3D model based on finite volume method describing the region of the surgical connection and a 0D model, based on a lumped parameter description of the remaining of the circulation. Both 3D and 0D patient-specific models used in the present study were developed in our previous work [10], and refer to a 4-year-old male patient who had undergone a BCPA. The novelty of the present work is the inclusion of a respiration model in the LPM, corresponding to the vessels of the body that are most affected by diaphragmatic movement.

2.1. 3D–0D preoperative model

A three-dimensional reconstruction of the BCPA anatomy was created from MR DICOM images using a custom version of the SimVascular package (http://simtk.org) (Fig. 2a). A tetrahedral mesh was generated to discretize the model, using Ansys ICEM 13.0 (Ansys Inc., Canonsburg, PA, USA). A mesh size of about 640,000 cells was used, according to a preliminary grid sensitivity analysis, where the mesh density was progressively increased (from about 160,000 to about 1,200,000 elements), accepting differences in the pressure drop between inlets and outlets lower than 1% in two subsequent grids.

The LPM of the whole pre-operative circulatory network, depicted in Fig. 2a, is comprised of different blocks to describe the heart, the systemic (including upper body and lower body, comprised of thoracic cavity, abdomen and legs) and pulmonary circulation. The pulmonary impedance is described by patient-specific RCR blocks [11], connecting the outlets of the 3D BCPA and

Please cite this article in press as: A. Baretta, et al., Respiratory effects on hemodynamics in patient-specific CFD models of the Fontan circulation under exercise conditions, European Journal of Mechanics B/Fluids (2012), doi:10.1016/j.euromechflu.2012.01.012

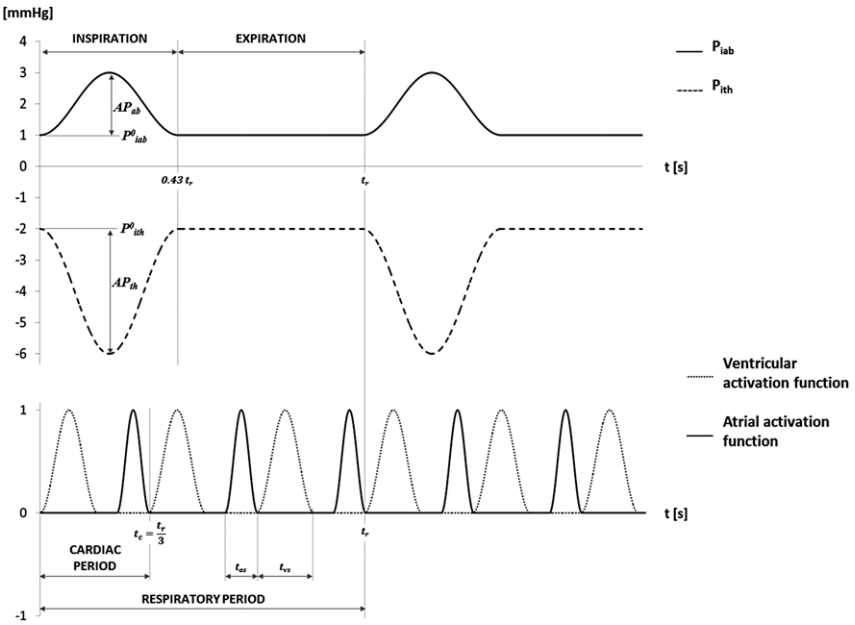

Fig. 3. Time tracings of extravascular intra-abdominal (solid line) and intra-thoracic (dashed line) pressures (upper panel); time tracings of ventricular (dotted line) and atrial (solid line) activation functions. The inspiration time is equal to 0.43 times the respiratory period (t_r), while the duration of a cardiac cycle (t_c) is 1/3 of the respiratory period t_{vs} and t_{as} are the durations of ventricular and atrial systole, respectively.

TCPC models to the single atrium, as illustrated in Fig. 2b. The heart was described by two contracting chambers: a single atrium and a single ventricle. The contraction was regulated by two activation functions, shifted in time (Fig. 3) [12]. The parameters values were obtained on the basis of the available preoperative clinical mean values and waveforms (i.e., MR flow tracings, catheterization derived pressure tracings and echocardiographic Doppler velocity tracings) as described in detail in [10]. In particular, a heart rate of 84 bpm, a body surface area (BSA) of 0.66 m^2, pulmonary and systemic vascular resistances (PVR and SVR) of 5.3 WU and 35 WU (Wood units, WU. 1WU $=$ 7999.2 Pa s l^{-1}), respectively, were adopted.

The LPM resulted in an algebraic-differential equation system; the coupling between LPM and 3D model was achieved by means of user-defined functions written in C++ language, implemented in Ansys Fluent 13.0 (Ansys Inc., Canonsburg, PA, USA). The LPM differential equation system was solved with the explicit Euler method, while the Navier–Stokes equations were solved within the 3D domain with the SIMPLE (Semi-Implicit Method for Pressure-Linked Equations) algorithm, using for both a time step of 0.0005 s. In our coupling framework the exchange of information occurs at the boundary sections of the 3D domain, once per time step: the 0D model calculates pressures over the compliances that are imposed with a uniform profile at each boundary section of the 3D domain, which in turn calculates the flow rates through the boundary sections used as forcing terms for the 0D network [13]. The blood was assumed to be a Newtonian fluid, with a viscosity of 0.004 kg (m s)$^{-1}$ and a density of 1060 kg m^{-3}. Rigid walls were assumed for the 3D portion of the model.

2.2. 3D–0D postoperative models

Starting from the preoperative 3D model, three different postoperative TCPC configurations were created using virtual surgery techniques [6]: a traditional *T*-junction with no offset between the venae cavae (T-TCPC), a configuration with an offset towards the LPA (O-TCPC), and a *Y*-graft connection of the main branches (Y-TCPC) [8,14] (Fig. 2c–e). About 720,000 mesh elements were used.

Each outlet of the 3D models was connected to a RCR pulmonary block, the IVC was disconnected from the atrium and connected to the IVC inlet section of the 3D, as shown in Fig. 2c for the O-TCPC model.

The simulation settings and assumptions are previously described (see Section 2.1).

2.3. Respiration model

To reproduce the respiratory effects on the circulation, extravascular pressure generators were included in the thoracic and abdominal cavities, namely intra-thoracic and intra-abdominal pressure generators (P_{ith} and P_{iab}, respectively), connected to the vascular compliances of the thoracic and abdominal blocks.

The rhythm of inspiration and expiration was represented by a periodic function of time *AR(t)*, indicated as respiratory activation function, which oscillates between 0 and 1 and causes an overpressure in the abdomen and a lower pressure in the thoracic cavity during inspiration, similarly to the pressure waveforms used in [15].

External pressures P_{ith} and P_{iab} vary in time according to functions (1) and (2):

$$P_{ith}(t) = AR(t) \cdot AP_{th} + P^0_{ith} \tag{1}$$

$$P_{iab}(t) = AR(t) \cdot AP_{ab} + P^0_{iab} \tag{2}$$

where AP_{th} and AP_{ab} are the maximum amplitude variation of the two pressures, while P^0_{ith} and P^0_{iab} are the baseline pressure values. These transmural pressures act in sync, the former negatively and the latter positively, as shown in Fig. 3.

Briefly, the respiratory frequency f_r was defined as 1/3 of the heart rate in both rest and exercise conditions. An exact submultiple of the heart rate was assumed for f_r in order to reduce the computational time cost, since a whole number of cardiac and respiratory cycles is required for the results analysis.

The value adopted for the respiratory systole, i.e., the period in which the $AR(t)$ is non-zero, was set to 0.43 times the respiratory period t_r, calculated as $1/f_r$. The values of AP_{th}, AP_{ab}, P^0_{ith} and P^0_{iab} were set to -4, 2, -2 and 1 mm Hg, respectively.

Please cite this article in press as: A. Baretta, et al., Respiratory effects on hemodynamics in patient-specific CFD models of the Fontan circulation under exercise conditions, European Journal of Mechanics B/Fluids (2012), doi:10.1016/j.euromechflu.2012.01.012

Table 1
Values of quantities adopted in the simulations at rest and exercise conditions. HR, heart rate; f_r, respiratory frequency; PVR, pulmonary vascular resistances; SVR, systemic vascular resistances.

	Rest (BCPA)	Exercise (TCPC)
HR (bpm)	84	168
f_r (bpm)	28	56
PVR (WU)	5.3	3.2
SVR (WU)	35.0	23.5

2.4. Multiscale model simulations

As a first step, rest conditions were simulated for the preoperative model to compare the results, including the respiratory model, with the clinical tracings acquired preoperatively.

Second, the three different TCPC options were tested under exercise conditions, since minor differences were previously [10] detected among models at rest.

The exercise conditions were achieved by doubling the heart and respiratory rate, reducing PVR by 40%, and the whole SVR by 33% [16]. The decrease in SVR was obtained by reducing leg resistances by 85%, thus simulating lower limb exercise.

More precisely, when exercise is simulated the vessels are assumed to vasodilate (i.e., they increase their diameter) thus decreasing the resistance and increasing the compliance. Considering the dependence of the parameters on the diameter ($R \approx D^{-4}$ and $C \approx D^3$, [17]), and leaving other factors unchanged (e.g., the wall thickness), the compliances C_{i-exe} of the lung and leg blocks in exercise conditions were obtained according to Eq. (3):

$$C_{i-exe} = C_i \left(\frac{R_{i-exe}}{R_i} \right)^{-3/4}, \tag{3}$$

where C_i, R_i are the compliances and resistances of the lung and leg blocks of the model at rest conditions, and R_{i-exe} are the resistances of the lung and leg blocks of the model under exercise conditions.

Values of quantities used in rest and exercise conditions are listed in Table 1.

Transient simulations for each model were run on an IntelR Core i7 (3 GHz) processor, with a 64 bit operating system. The multiscale simulations required a CPU time expenditure of approximately 4 days per respiratory cycle.

2.5. Post-processing of results

Postoperative models were compared on the basis of local and global variables, namely the energy efficiency η and power losses $\dot{W}_{DISS}$ of each geometry, the flow split between right and left lungs, cardiac output (CO), SVC and IVC flows, and pulsatility flow index (*PFI*).

Power losses $\dot{W}_{DISS}$ and energy efficiency η of the TCPC geometries were calculated as follows (Eqs. (4)–(7)):

$$\dot{W}_{IN} = Q_{IVC} \left(p_{IVC} + \frac{1}{2}\rho V_{IVC}^2 \right) + Q_{SVC} \left(p_{SVC} + \frac{1}{2}\rho V_{SVC}^2 \right) \tag{4}$$

$$\dot{W}_{OUT} = \sum_i Q_{LPAi} \left(p_{LPAi} + \frac{1}{2}\rho V_{LPAi}^2 \right) + \sum_i Q_{RPAi} \left(p_{RPAi} + \frac{1}{2}\rho V_{RPAi}^2 \right) \tag{5}$$

$$\dot{W}_{DISS} = \dot{W}_{IN} - \dot{W}_{OUT} \tag{6}$$

$$\eta = \frac{\dot{W}_{OUT}}{\dot{W}_{IN}} \tag{7}$$

where $V^2_{L(R)PAi}$, $p_{L(R)PAi}$ and $Q_{L(R)PAi}$ are the mean square velocity, pressure and flow over the i-th outlet section of the left (or right) side of the model.

Moreover, in order to quantify the time dependence of venous flows due to both cardiac pulsatility and respiratory effects, a dimensionless index of pulsatility was calculated in Eq. (8):

$$PFI = \frac{(Q_{\max} - Q_{\min})}{Q_{mean}} \tag{8}$$

where $Q_{\max}$ is the peak positive flow rate, and $Q_{\min}$ is the minimum forward flow in unidirectional flow, or the maximum negative flow rate in flow reversal, both calculated within a respiratory cycle; Q_{mean} is the flow rate averaged over one respiratory cycle.

3. Results and discussion

3.1. 3D–0D preoperative model

We first compare the pre-operative multiscale model results to the clinical tracings acquired on the patient preoperatively.

Fig. 4 shows the model flow rates in the hepatic vein (HV), IVC and SVC, which are representative of the venous behavior of the lower and upper body, respectively. These may be compared with those clinical time tracings for which respiration effects are evident. In fact, among the clinical data available for this patient, only Doppler tracings show the modulation of the respiration in normal conditions, i.e., free breathing (Fig. 5), while MR tracings were cardiac-gated and respiratory-compensated and catheterization tracings were acquired during mechanical ventilation.

In Figs. 4 and 5 the cardiac activity is displayed by the ventricular activation function in the model curves, and by the ECG in the clinical tracings. Despite the different units and assuming a constant cross section of the vessels, the main features of Doppler venous flows are well captured. In our previous work [10] good agreement was obtained for the BCPA model without respiration effects, between model results and the whole patient MR tracings (both arterial and venous).

In the present simulations, respiratory modulation of the model flow tracings can be observed in both venous curves, reflecting the behavior found in the clinical data, although the patient's HV tracing shows a respiratory period longer than that adopted in the model (four vs three times the cardiac period), due to the physiological variability of f_r.

Both Figs. 4 and 5 show typical events occurring in venous flows within cardiac and respiratory periods: two peaks and two valleys within a cardiac cycle, which are modulated according to the respiration. Moreover, in agreement with clinical tracings the model found that respiratory effects are manifest only for lower veins (IVC and HV), whereas the SVC flow exhibits a slight pulsatility due to cardiac pulsatility with no clear respiratory modulation. The model flow waveforms show higher pulsatility for HV compared to SVC (PFI of 5.88 vs. 0.63), in good agreement with the clinical velocity tracings. Furthermore, the model waveform for the IVC flow (Doppler tracing not available) shows a 6.65 PFI, greater than that of the SVC flow, confirming the higher pulsatility previously observed in the model without the respiratory effects [10]. This underlines that IVC pulsatility results mainly from cardiac contractility (in particular atrial filling, contraction and emptying), corresponding with its direct connection to the atrium. Conversely, SVC is less affected by atrial events because of the interposition of lung vasculature in the BCPA configuration.

Please cite this article in press as: A. Baretta, et al., Respiratory effects on hemodynamics in patient-specific CFD models of the Fontan circulation under exercise conditions, European Journal of Mechanics B/Fluids (2012), doi:10.1016/j.euromechflu.2012.01.012

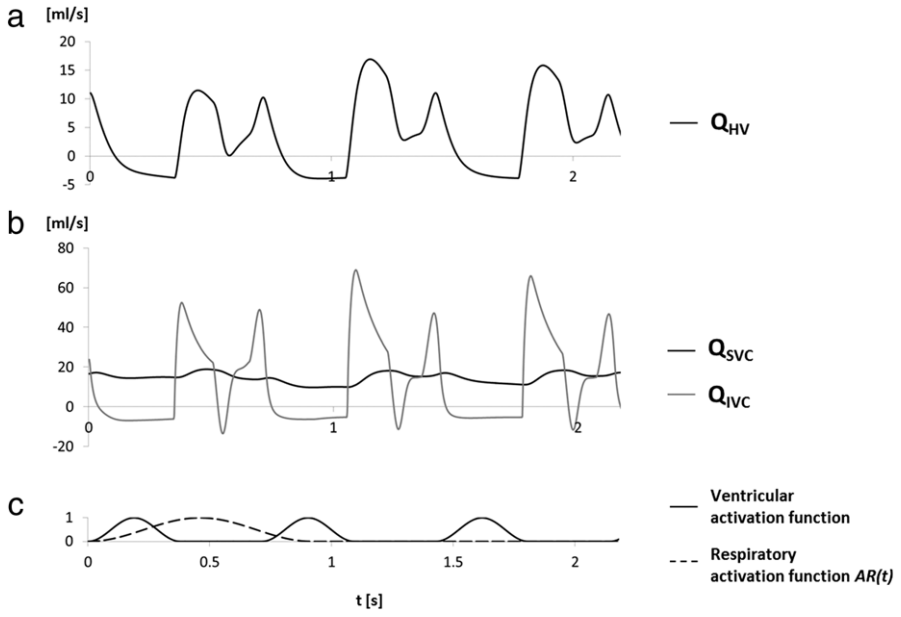

Fig. 4. Preoperative state model tracings of (a) HV and (b) SVC and IVC flows; (c) ventricular (solid line) and respiratory (dashed line) activation functions.

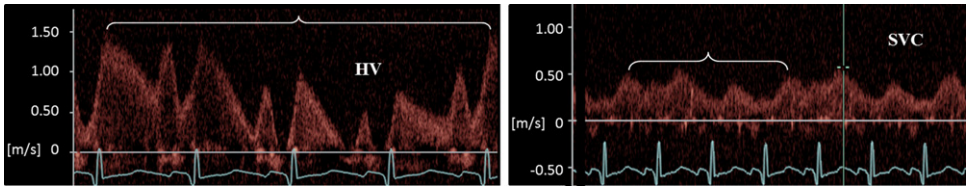

Fig. 5. Doppler tracings of hepatic vein (left) and SVC (right) velocities. A respiratory frequency of about 1/3 and 1/4 of the cardiac frequency can be appreciated in SVC and HV tracings, respectively. Braces indicate the respiratory period.

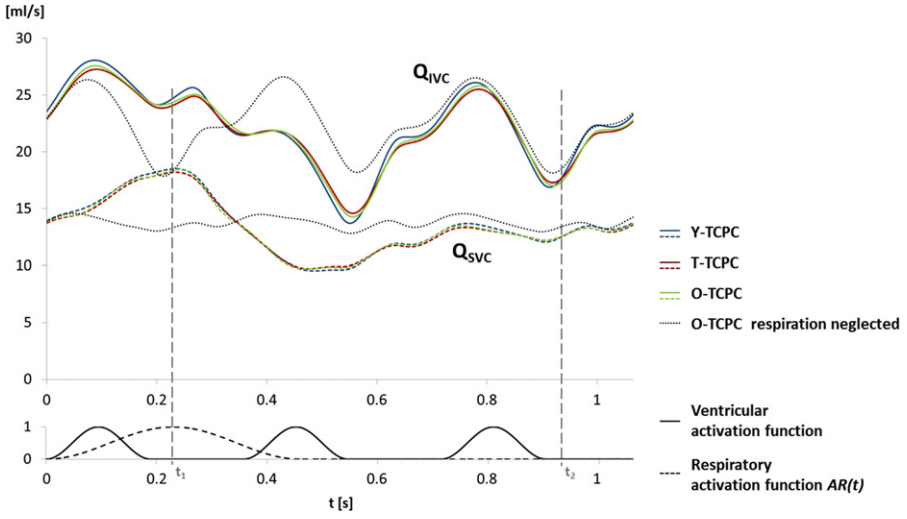

Fig. 6. SVC (dashed line) and IVC (solid line) flow tracings of post-operative configurations T-TCPC, O-TCPC and Y-TCPC. SVC and IVC flow tracings in absence of the respiration [10] (dotted lines) are reported only for the O-TCPC model. The ventricular (solid line) and respiratory (dashed line) activation functions are reported. Instants t_1 and t_2 where fluid dynamic velocity is analyzed in Fig. 7 are depicted.

3.2. 3D–0D postoperative models in exercise conditions

The three different TCPC configurations tested in exercise conditions produce the flow tracings depicted in Fig. 6. In the same graph, SVC and IVC flow tracings in absence of respiration [10] are reported too, only for the O-TCPC model (indeed, differences less than 1% were previously detected among models).

Similarly, the curves of the three tested cases roughly overlap, showing no remarkable differences among the models.

In the resulting tracings, we observe respiratory modulation, with quite high PFI values, ranging from 0.61 (for the T-TCPC) to 0.69 (for the Y-TCPC) and from 0.57 (for the T-TCPC) to 0.65 (for the Y-TCPC) in the SVC and IVC, respectively. On the contrary, in the O-TCPC model tested without respiration the PFI value in the SVC

Please cite this article in press as: A. Baretta, et al., Respiratory effects on hemodynamics in patient-specific CFD models of the Fontan circulation under exercise conditions, European Journal of Mechanics B/Fluids (2012), doi:10.1016/j.euromechflu.2012.01.012

Table 2
Values of flow rates, power loss and energy efficiency for the TCPC multiscale models under exercise conditions, averaged over each cardiac cycle.

Cardiac cycle	T-TCPC			O-TCPC			Y-TCPC		
	1st	2nd	3rd	1st	2nd	3rd	1st	2nd	3rd
CO (ml/s)	40.9	30.4	34.7	41.2	30.4	34.8	41.6	29.3	35.1
Q_{RPA}/CO	0.63	0.62	0.63	0.62	0.63	0.61	0.62	0.65	0.62
Q_{SVC}/CO	0.39	0.36	0.37	0.39	0.36	0.37	0.39	0.38	0.37
$\dot{W}_{DISS}$ (mW)	6.9	3.2	4.4	6.2	2.8	3.9	4.9	2.1	3.1
η(%)	88.8	93.9	92.4	89.9	94.5	93.1	92.1	95.9	94.6

(CO = Cardiac output; Q = flow rate; RPA = right pulmonary artery; SVC = superior vena cava; $\dot{W}_{DISS}$ = power loss; η = energy efficiency).

Table 3
Values of flow rates, power loss and energy efficiency for the TCPC multiscale models under exercise conditions. The previous model results where respiration was neglected (left columns) [10] are compared with the present model results (right columns), where respiration is included (values are averaged over a respiratory cycle).

Respiration	T-TCPC		O-TCPC		Y-TCPC	
	Neglected	Included	Neglected	Included	Neglected	Included
CO (ml/s)	37.5	35.3	37.1	35.5	37.6	35.7
Q_{RPA}/CO	0.62	0.63	0.62	0.62	0.62	0.62
Q_{SVC}/CO	0.37	0.38	0.37	0.38	0.38	0.38
$\dot{W}_{DISS}$ (mW)	4.8	4.7	4.4	4.3	3.4	3.3
η(%)	91.9	91.8	92.7	92.6	94.4	94.2

(CO = Cardiac output; Q = flow rate; RPA = right pulmonary artery; SVC = superior vena cava; $\dot{W}_{DISS}$ = power loss; η = energy efficiency).

was very low (0.12), whereas IVC kept notable cardiac pulsatility (PFI equal to 0.36).

Both the SVC and IVC flow tracings show different features in the three cardiac cycles included in a single respiratory cycle, since each of them occurs during a different respiratory phase: the first is entirely within the inspiration, the second lies across inspiration and expiration, whereas the third cycle occurs during expiration.

Higher flow values were obtained within the first cardiac cycle, whereas in the second cycle lower values are evident. The third cycle show intermediate values, and stronger similarity with the tracings where the respiration is neglected (Fig. 6).

According to the model, an opposite respiratory modulation can be noticed in the pre-operative scenario: lower flow values were detected during the first cardiac cycle, while higher flow values were noticed during the second cardiac cycle (Fig. 4). So far, no prior literature work has investigated the effect of the respiration on caval flows in different cardiac cycles in BCPA patients. Hence, this evidence has to be confirmed.

In Table 2 values of flows, power loss and energy efficiency are averaged over each of the three cardiac cycles occurring in a respiratory cycle, allowing an overview on how fluid dynamic variables change during respiration.

As already observed in Fig. 6, higher flow values are detected during inspiration (1st cardiac cycle), consistent with previous works on the effects of the respiration on venous return in TCPC patients [5,18]. In general, the descent of the diaphragm during inspiration causes an augmented positive intra-abdominal pressure and a reduced negative intra-thoracic pressure, thus enhancing the venous return through the IVC. In TCPC patients the dependence of IVC flow on respiration is even higher, since the HV flow, which constitutes the majority (nearly 40%) of the inferior venous return, is strongly related to the respiration (55% of respiratory-dependent flow) [18]. However, regardless the model, the pulmonary flow split does not change considerably during the respiratory cycle (differences <5%), with a higher amount of flow directed towards the right lung. In general, the fraction of cardiac output coming from the upper body (Q_{SVC}/CO) is lower than 0.5, indicating a dominant IVC flow during each cardiac cycle. Moreover, results show a greater variation of flow rates during the respiratory cycle than between the 3 different geometries at a given point in time.

Additionally, for all the surgical options, as a consequence of the above described flow rates, the first and the second cardiac cycles resulted to be the most and the less dissipative, respectively. Nevertheless, all the values of η are higher than 88%.

Fig. 7 shows the velocity-colored pathlines in the three TCPC options, comparing two time instants of the respiratory cycle (see Fig. 6) corresponding to the same instant of the cardiac cycle, one during inspiration ($t_1 = 0.22$ s, middle column) and one during expiration ($t_2 = 0.93$ s, right column), with the equivalent instant in the model without respiration (left column) [10].

For a fixed TCPC model, similar caval flow trajectories can be appreciated during the different instants. Nevertheless, the interactions between SVC and IVC flows are peculiar according to different surgeries. When comparing the "inspiration" and "expiration" phases, an increase in flow velocity during the former is evident, in agreement with flow rates reported in Fig. 6 and Table 2, with values close to 0.50 m/s in the pulmonary branches bifurcations. Moreover, similarities can be noticed between "no respiration" and "expiration" scenarios, in terms of pathline colors and patterns, consistently with Fig. 6 where the caval flow tracings of the two scenarios were roughly overlapped during expiration.

In Table 3 the fluid dynamic variables are averaged over a respiratory cycle and compared to those obtained without respiration in our previous work [10].

On average, the cardiac output is slightly lower (≈5%) than that obtained previously in the models where respiration was disregarded. Nevertheless, the splitting between upper/lower body and right/left lung remains unchanged from the case analyzed previously.

Moreover, as occurred in the models without respiration, small differences (<3%) can be observed among flow values averaged over a respiratory cycle and power losses obtained in the different models. This occurrence indicates that the effect of the inclusion of a respiratory model has small influence on the hemodynamics of the Fontan circulation, without any enhancement of differences in the behaviors of various investigated surgeries. Nevertheless, it is also possible that inclusion of these effects will result in large differences in local quantities not currently investigated, like temporal changes of wall shear stress which for other vascular regions were associated to an anomalous response of the vessel wall [19].

The models follow the same trend as in absence of respiration, with the T-TCPC model reporting the lowest values of flow rates and energy efficiency, while the Y-TCPC model reports the highest mean values of flows and energy efficiency among the models.

Please cite this article in press as: A. Baretta, et al., Respiratory effects on hemodynamics in patient-specific CFD models of the Fontan circulation under exercise conditions, European Journal of Mechanics B/Fluids (2012), doi:10.1016/j.euromechflu.2012.01.012

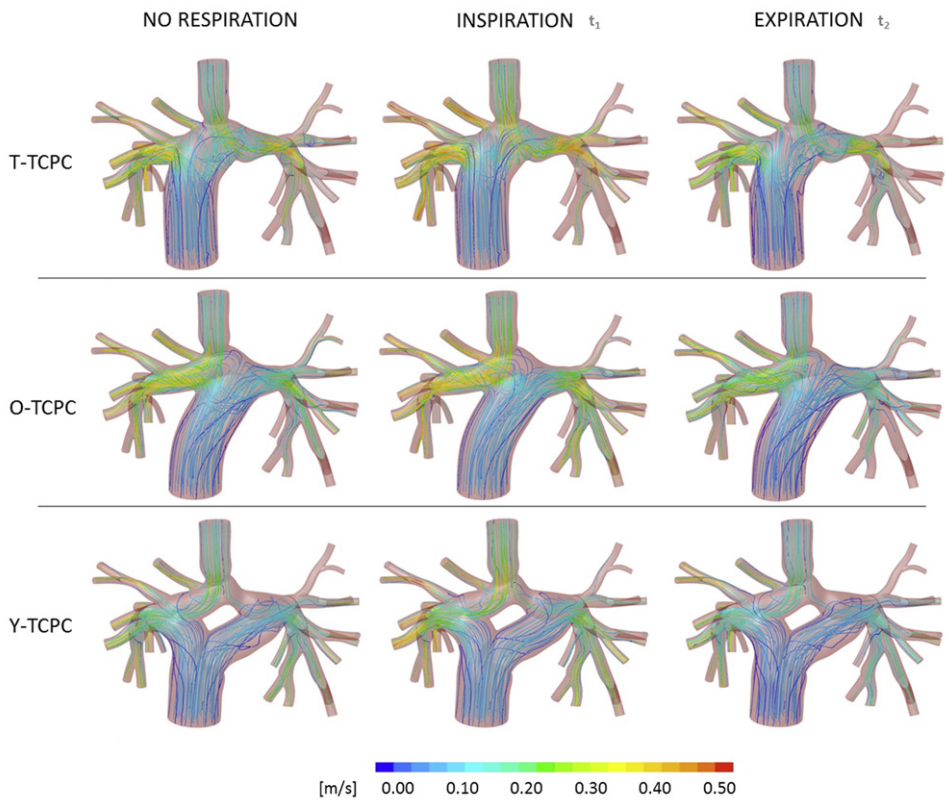

Fig. 7. Velocity-colored pathlines in T-TCPC, O-TCPC, Y-TCPC tested in exercise conditions, without the respiratory model (left), during inspiration (middle) and during expiration (right).

Moreover, all the models showed energy efficiency values over 90%, suggesting that the Fontan circulation is barely affected by the TCPC geometry, while pulmonary and systemic resistances have the most impact on the overall hemodynamics.

4. Conclusions

In this study, we have extended our previous work to include effects of respiration in 3D–0D models of one pre-operative and three different post-operative models, by including an effective, although simple, model of the respiration that simulates the varying extravascular thoracic and abdominal pressures. In contrast to previous works [4,6,8], the multiscale approach enables automatic derivation of oscillations in the caval flow that result from respiration, through the action of extravascular pressure generators.

The results using this approach confirm that the model realistically reproduces clinically observed venous time tracings. Namely, simulations showed an evident respiratory modulation of flows, with a slight decrease in local energy efficiency compared to the case devoid of the respiration.

While we do not observe any significant differences in global hemodynamics with and without respiration, inclusion of these effects results in greater physiologic realism. Although respiratory effects require longer computational time, this can be compensated for by an increase in computing power for future application in a clinically relevant time frame.

Finally, the 3D part of the multiscale model showed local distortions and interactions of SVC and IVC flow. Therefore, such a coupled model could be adopted when local hemodynamics of the connection are investigated, i.e., SVC and IVC flow waveforms and interactions.

Future work could include in the model the gravity and peripheral muscular pump contributions [18,20] that may affect venous return in Fontan circulation, particularly when tested in exercise conditions. Moreover, temporal changes of local fluid dynamic variables, like wall shear stress, should be further investigated.

An extension of these results to models based on a larger group of patients is needed to further confirm our findings.

Acknowledgments

This study was supported by a grant from the Fondation Leducq, Paris, France.

The authors acknowledge Dr. Jeffrey A. Feinstein, Guillaume Troianowski and Weiguang Yang for their contributions.

References

[1] A.M. Gaca, J.J. Jaggers, L.T. Dudley, G.S. Bisset III, Repair of congenital heart disease: a primer–Part 1, Radiology 247 (3) (2008) 617–631.
[2] F. Migliavacca, M.R. de Leval, G. Dubini, R. Pietrabissa, R. Fumero, Computational fluid dynamic simulations of cavopulmonary connections with an extracardiac lateral conduit, Med. Eng. Phys. 21 (1999) 187–193.
[3] F. Migliavacca, G. Dubini, E.L. Bove, M.R. de Leval, Computational fluid dynamics simulations in realistic 3-d geometries of the total cavopulmonary anastomosis: the influence of the inferior caval anastomosis, J. Biomech. Eng. 125 (2003) 805–813.
[4] A.L. Marsden, I.E. Vignon-Clementel, F.P. Chan, J.A. Feinstein, C.A. Taylor, Effects of exercise and respiration on hemodynamic efficiency in CFD simulations of the total cavopulmonary connection, Ann. Biomed. Eng. 35 (2007) 250–263.
[5] V.E. Hjortdal, K. Emmertsen, E. Stenbøg, T. Fründ, M. Rahbek Schmidt, O. Kromann, K. Sørensen, E.M. Pedersen, Effects of exercise and respiration on blood flow in total cavopulmonary connection: a real-time magnetic resonance flow study, Circulation 108 (2003) 1227–1231.
[6] W. Yang, I.E. Vignon-Clementel, G. Troianowski, V.M. Reddy, J.A. Feinstein, A.L. Marsden, Hepatic blood flow distribution and performance in traditional and Y-graft Fontan geometries: a case series computational

fluid dynamics study, J. Thorac. Cardiovasc. Surg. (published on-line, doi:10.1016/j.jtcvs.2011.06.042) (in press).
[7] O. Dur, C.G. DeGroff, B.B. Keller, K. Pekkan, Optimization of inflow waveform phase-difference for minimized total cavopulmonary power loss, J. Biomech. Eng. 132 (3) (2010) 031012.
[8] A.L. Marsden, A.J. Bernstein, V.M. Reddy, S.C. Shadden, R.L. Spilker, F.P. Chan, C.A. Taylor, J.A. Feinstein, Evaluation of a novel Y-shaped extracardiac Fontan baffle using computational fluid dynamics, J. Thorac. Cardiovasc. Surg. 137 (2009) 394–403.
[9] A. Quarteroni, A. Veneziani, Analysis of a geometrical multiscale model based on the coupling of PDE's and ODE's for blood flow simulations, Multiscale Model. Simul. 1 (2003) 173–195.
[10] A. Baretta, C. Corsini, W. Yang, I.E. Vignon-Clementel, A.L. Marsden, J.A. Feinstein, T.-Y. Hsia, G. Dubini, F. Migliavacca, G. Pennati, The modeling of congenital hearts alliance (Mocha) investigators, virtual surgeries in patients with congenital heart disease: a multi-scale modelling test case, Phil. Trans. R. Soc. A 369 (2011) 4316–4330.
[11] G. Troianowski, C.A. Taylor, J.A. Feinstein, I.E. Vignon-Clementel, Three-dimensional simulations in Glenn patients: clinically based boundary conditions, hemodynamic results and sensitivity to input data, J. Biomech. Eng. 133 (11) (2011) (in press).
[12] F. Migliavacca, G. Pennati, G. Dubini, R. Fumero, R. Pietrabissa, G. Urcelay, E.L. Bove, T.-Y. Hsia, M.R. de Leval, Modeling of the Norwood circulation: effects of shunt size, vascular resistances, and heart rate, Am. J. Physiol. Heart Circ. Physiol. 280 (5) (2001) H2076–H2086.
[13] F. Migliavacca, R. Balossino, G. Pennati, G. Dubini, T.-Y. Hsia, M.L. de Leval, E.L. Bove, Multiscale modelling in biofluidynamics: Application to reconstructive paediatric cardiac surgery, J. Biomech. 39 (2006) 1010–1020.
[14] W.G. Yang, J.A. Feinstein, A.L. Marsden, Constrained optimization of an idealized Y-shaped baffle for the Fontan surgery at rest and exercise, Comput. Methods Appl. Mech. Eng. 199 (2010) 2135–2149.
[15] M.F. Snyder, V.C. Rideout, Computer simulation studies of the venous circulation, IEEE Trans. Biomed. Eng. 16 (4) (1969) 325–334.
[16] K.S. Sundareswaran, K. Pekkan, L.P. Dasi, K. Whitehead, S. Sharma, K.R. Kanter, M.A. Fogel, A.P. Yoganathan, The total cavopulmonary connection resistance: a significant impact on single ventricle hemodynamics at rest and exercise, Am. J. Physiol. Heart Circ. Physiol. 295 (6) (2008) H2427–H2435.
[17] G. Pennati, R. Fumero, Scaling approach to study the changes through the gestation of human fetal cardiac and circulatory behaviors, Ann. Biomed. Eng. 28 (2000) 442–452.
[18] T.-Y. Hsia, S. Khambadkone, A.N. Redington, F. Migliavacca, J.E. Deanfield, M.R. de Leval, Effects of respiration and gravity on infradiaphragmatic venous flow in normal and Fontan patients, Circulation 102 (2000) III148–III153.
[19] A.M. Malek, S.L. Alper, S. Izumo, Hemodynamic shear stress and its role in atherosclerosis, J. Am. Med. Assoc. 282 (21) (1999) 2035–2042.
[20] T.W. Rowland, The circulatory response to exercise: role of the peripheral pump, Int. J. Sports Med. 22 (8) (2001) 558–565.

Please cite this article in press as: A. Baretta, et al., Respiratory effects on hemodynamics in patient-specific CFD models of the Fontan circulation under exercise conditions, European Journal of Mechanics B/Fluids (2012), doi:10.1016/j.euromechflu.2012.01.012